G. Arutinov et al., "Dynamics of capillary self-alignment for mesoscopic foil devices"

Supplementary Information

1. Dissipative viscous forces

The contribution of dissipative viscous forces was estimated according to Newton's Law of Viscosity (eq. 1):

$$F_{fric} = \eta S_{die} \frac{dv_z}{dz}, \qquad (1)$$

where η is the viscosity coefficient (for water at RT, $\eta_{water} = 0.975\ mPa \cdot s$), S_{die} the surface area of the die (for 18 × 18 mm^2 foil die, $S_{die} = 324\ mm^2$), and $\frac{dv_z}{dz}$ the vertical velocity gradient. With the assumption of linear vertical velocity gradient in the liquid layer (Fig. 1), eq. 1 could be expressed as:

$$F_{fric} = \eta S_{die} \frac{dv_z}{dz} = \eta S_{die} \frac{d\left(v_0 \frac{z}{h}\right)}{dz} = \eta S_{die} \frac{v_0}{h} = 0.52{\times}10^{-3}{\times}v_0\ (N), \qquad (2)$$

where v_0 is the velocity of the foil die (extracted from recorded data).

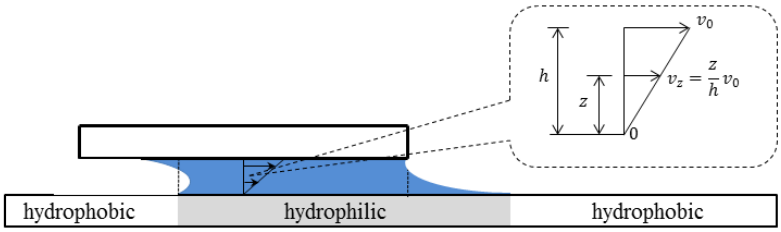

Fig. 1. Sketch of a misaligned foil die with a linear velocity gradient in the liquid layer

2. Sliding approximation

For large displacements from the equilibrium position, lateral capillary forces can be computed numerically through SE simulations, as well as analytically using a *sliding approximation* hereby proposed (Fig. 2). Assuming: 1) uniaxial displacement, 2) $u>>h$, 3) flat water/air interfaces, 4) negligence of water/air interfaces parallel to the direction of motion, and 5) a single unpinned triple contact line as shown in the letter, for a square or rectangular die the surface energy differential with respect to a uniaxial perturbation dx is given by:

$$dE = -Ldx\gamma_{SV} - Ldx\gamma_{LV} + Ldx\gamma_{SL}, \qquad (3)$$

where L is the length of the die side perpendicular to the direction of motion, and $\gamma_{SV}, \gamma_{LV}, \gamma_{SL}$ are the surface energies between die and air, water and air, and die and water, respectively. The restoring capillary force is then:

$$F_{slid} = -\frac{dE}{dx} = L(\gamma_{SV} - \gamma_{LV} + \gamma_{SL}) \qquad (4)$$

Using Young's equation $\gamma_{SV} = \gamma_{SL} + \gamma_{LV}\cos\theta$, θ being the liquid CA on the bottom surface of the die, we get:

$$F_{slid} = -L\gamma_{LV}(1 + \cos\theta) \qquad (5)$$

Note that $\lim_{\theta\to 0} F_{slid} = -2L\gamma_{LV}$, consistently with eq. 4 of ref. 5 (for $x = u \gg h$). That is, this model can be considered as an extension of the common geometrical model for the cases where the displacements of the die from equilibrium are large enough and die wettability such that triple contact line unpinning from the outer die edge takes place.

Adopting Young's equation amounts to assuming *static* equilibrium conditions for the meniscus. This condition does clearly *not* hold in a dynamic setting like the one investigated. This partly underlines the mismatch with actual data. Also, as is the case in our experimental case, we hereby assumed an asymmetrical condition whereby the CA water on the die is larger than on the binding site (here patterned in silicon dioxide, for which the CA of water tends to 0 (perfect wetting). If dewetting happens on the binding site, capillary SA is compromised.

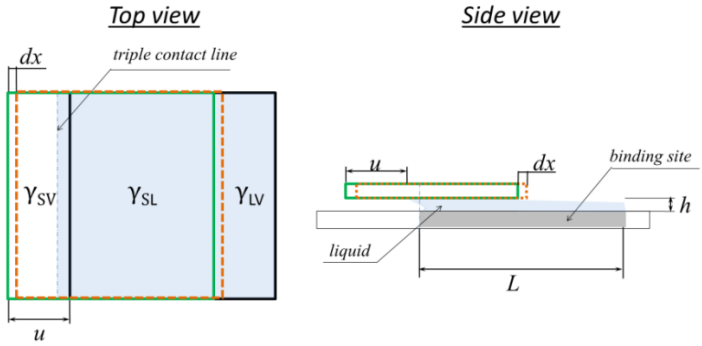

Fig 2. Top and side view sketches of the sliding approximation for a square die with {u}>>h.

3. Comparison of lateral capillary forces

For large displacements from equilibrium, lateral capillary forces acting on the dies were computed numerically through SE simulations, as well as analytically using a *sliding approximation* according to eq. 5 of the previous section. Table I compares the predictions with actual data gathered from acceleration of dies and their masses. As seen, the sliding model well matches the numerical predictions of SE. Still, both substantially overestimate the experimentally estimated values of the forces, even accounting for the viscous dissipative forces as discussed in the Letter. This was not unexpected given the quasi-static nature of both models.

Table I. Comparison of lateral capillary force obtained from experiments, SE calculations and analytical sliding approximation as function of different degrees of wettability parameterized by water CAs. Experimental results are obtained from acquired acceleration data for the parabolic regime (die: 0.80 mg/mm^2).

	Restoring force (mN)		
	Experimental data	Surface Evolver simulation	Sliding approximation
PEN hydrophobic	0.47	1.07	1.12
PEN untreated	0.66	1.78	1.84
PEN hydrophilic	0.87	2.55	2.58

4. Water contact line dynamics

The dynamics of the unpinned water triple contact line was tracked upon formation through the high-speed camera setup (as sketched in Fig. 1 of the Letter) concurrently with the lateral alignment dynamics of the die. Here below are snapshots from the acquired video recordings (available as Supporting Information) focusing on the contact line for the three kinds of surface treatments applied to the PEN foils.

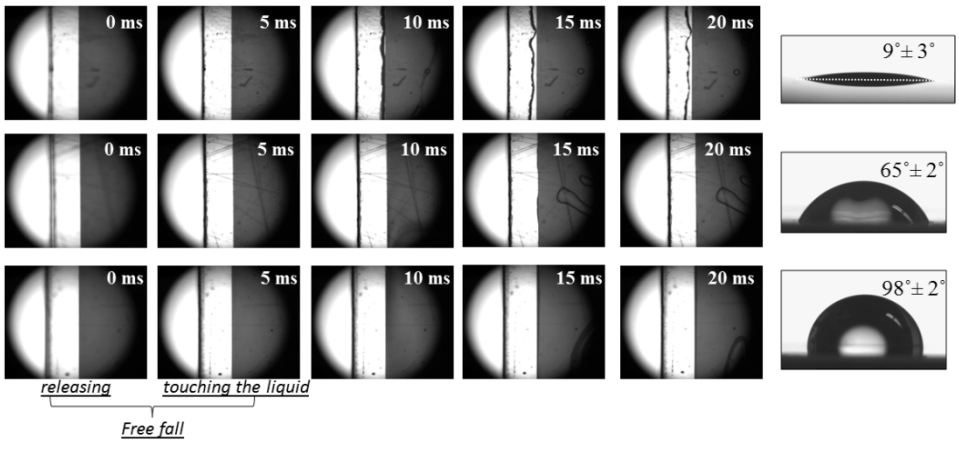

5. Self-alignment dynamics of a foil die

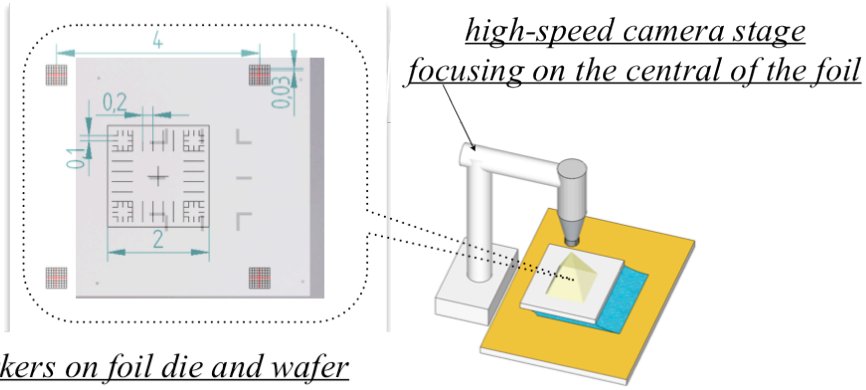

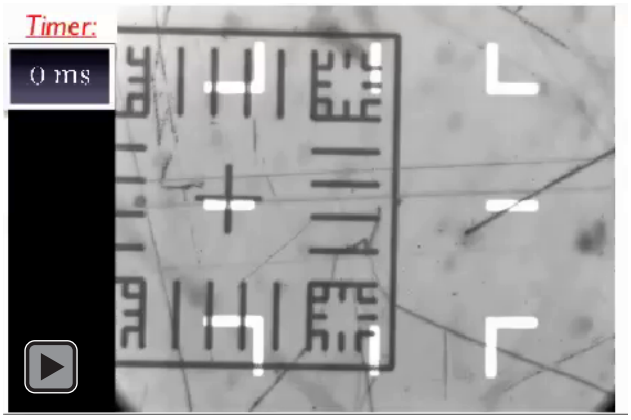

6. Uniaxial lateral self-alignment dynamics of a foil die and water contact line dynamics